ISSN 0001-4338, Izvestiya, Atmospheric and Oceanic Physics, 2022, Vol. 58, No. 6, pp. 625–634. © Pleiades Publishing, Ltd., 2022.

Statistical and Wavelet Transform-Based Study of the Latitudinal Ionospheric Response to an Annular Solar Eclipse on June 21, 2020

Devbrat Pundhir[a], *, Birbal Singh[b], **, and Rajpal Singh[c], ***

[a] *Seismo-electromagnetics and Space Research Laboratory (SESRL), Department of Physics, Raja Balwant Singh Engineering Technical Campus, Bichpuri, Agra, 283105 India*

[b] *Seismo-electromagnetics and Space Research Laboratory (SESRL), Department of Electronics and Communication, Raja Balwant Singh Engineering Technical Campus, Bichpuri, Agra, 283105 India*

[c] *Department of Physics, GLA University, Mathura, 281406 India*

**e-mail: devbratpundhir@gmail.com*

***e-mail: bbsagra@gmail.com*

****e-mail: rp.singh@gla.ac.in*

Received May 14, 2022; revised June 24, 2022; accepted August 11, 2022

Abstract—The ionosphere is a very complex and variable part of the atmosphere and it is controlled by solar activity. A solar eclipse is one of the phenomena which depicts a major impact on the ionosphere. In this study, we have analyzed the TEC data of 11 IGS-TEC stations (including one GPS station namely Agra) corresponding to a solar eclipse of June 21, 2020 for the duration of June 7–21, 2020. The TEC variations show lower values on the eclipse's day in comparison to the other days from the mean of each station except some of the stations like Agra (≈2 TECU), BHR4 (≈1TECU), IISC (≈0.5TECU) have shown the enhanced TEC variations. These results are examined by applying wavelet transform techniques such as continuous wavelet transforms (CWTs), and wavelet decomposition over the average, addition, and multiplication of TEC data of 11 stations for the duration of 9:30 AM to 3:30 PM on the eclipse's day. These results match very well with our statistical results and depict a better representation of the TEC variations during the solar eclipse. The wavelet decomposition of TEC variation has provided that TEC is affected by solar eclipse globally. These TEC variations are interpreted in terms of the mechanisms available in the literature.

Keywords: Solar eclipse, ionosphere, GPS, IGS, TEC, wavelet transform etc

DOI: 10.1134/S0001433822060196

1. INTRODUCTION

The ionosphere is a complex and highly variable region of the atmosphere that is affected by a slight change in any of its parameters [1]. The solar eclipse is one of the important solar-terrestrial events which directly controls the earth's ionosphere as a result of which the radio communication system is affected [2, 3]. A solar eclipse occurs when the Moon lies in between the Sun and the Earth and the sun's radiations are blocked by its shadow. The impact of the solar eclipse can be observed on the ionosphere in different dimensions i.e. Geographic latitude and longitude, geomagnetic activity, solar activity periods, local time, etc [4, 5]. The first report of an ionospheric study of the solar eclipse was provided in the early 20th century [6]. Later, numerous researchers examined the ionospheric response of solar eclipse using GPS and satellite-based measurements [7–16]. These studies have shown a reduction in electron density due to solar eclipse and it is possible because of the fast reduction in solar EUV flux. Additionally, the impact of the December 26, 2019 annular solar eclipse (ASE) on meteorological parameters and the land surface temperature has also been investigated and found significant effect in the southeastern Arabian Peninsula region [16]. Researchers have also studied ionospheric response to solar eclipse using different numerical simulation and modeling techniques [12, 17, 18]. Different methods have been used to analyze ionospheric TEC data and found significant results [4, 13–16]. Recently, researchers have reported the effect of the annular solar eclipse of June 21, 2020 on ionospheric TEC variations. [19] examined the impact of a solar eclipse on August 21, 2017 in form of ionospheric bow waves induced by the solar eclipse by using a dense network of Global Navigation Satellite System receivers at ~2.000 sites in North America. They also detected the large ionospheric perturbations moving

at the supersonic speed of the maximum solar obscuration which is too fast to be associated with known gravity waves or large-scale traveling ionospheric disturbance processes. [20] investigated the effect of a total solar eclipse in the Southeast Asia-Pacific region on March 9, 2016 on TEC data recorded at low latitude 40 GPS stations in Indonesia and found a reduction in the data which is directly proportional to the magnitude of the solar eclipse. More recently, [15] examined the ionospheric effects of the same eclipse on 9 March 2016 by using TEC and foF_2 data. They have found a significant reduction in the data. However, a thorough study of the effect of the solar eclipse on the ionosphere based on multiple station data and statistical analysis has not been done yet.

In this paper, first time, we have analyzed TEC data of 11 IGS stations including GPS station Agra corresponding to the annular solar eclipse of June 21, 2020 for the period of June 7–21, 2020 by using well-established statistical techniques as well as by using wavelet tools like wavelet transform, wavelet decomposition of the signal, etc. to highlight the nonlinear features of the TEC data which characterize its impact on latitudinal ionospheric variability. This solar eclipse was first noticed at Congo in Africa which passed through South Sudan, Ethiopia, Yemen, Oman, Saudi Arabia, the Indian Ocean, and Pakistan, before entering India over Rajasthan and then it moved to Tibet, China, Taiwan, before ending at the middle of the Pacific Ocean. To examine the effect of this solar eclipse, TEC stations are selected in such a manner that most of the stations lie on the path of the eclipse, and further solar (F10.7cm and sunspot numbers) and geomagnetic (∑Kp and Dst Indices) activity parameters and obscuration and magnitude of this annular solar eclipse have also been investigated.

2. EXPERIMENTAL

The IGS stations data have been downloaded from the website http://garner.ucsd.edu/pub/rinex/ and GPS data recorded at Agra station are considered. The IGS stations data are available in the public domain for research purposes under the observation of NASA. These stations are located over the globe and provide accurate and useful information on the impact of any event which affects the atmosphere. These 11 datasets (10 IGS and 1 GPS) are analyzed for the duration of June 7–21, 2020 by using statistical techniques such as mean, median, etc. and further TEC data have been analyzed by using wavelet transformation to ascertain the impact of the solar eclipse. To highlight the nonlinear features of the data, the average, addition, and multiplication of TEC data of all the stations have been computed on the eclipse's day under its period of occurrence i.e. 09:30 AM to 03:30 PM (Local Time) and wavelet transform (WT) has been performed on the same by using the wavelet tool available in MATLAB. Wavelet transform is a contemporary nonlinear data processing tool that is one of the most useful methods to analyze the non-stationary signals in the frequency domain [21]. Here, the signal is analyzed in low and high-frequency parts. In the high-frequency part, high time and low-frequency resolutions are used while in the low-frequency part, low time and high-frequency resolutions are used. In brief, the continuous wavelet transform (CWT) is the measure of resemblance between a signal and an analyzing function. The CWT can compare the signal to shifted and compressed or stretched versions of a wavelet which provides a better representation of the signal and unhide the useful information in the signal. The mathematical details of wavelet transform are given by [22].

In the mathematics, a wavelet is a series of functions $\Psi_{u,s}(t)$ which is computed from a function $\Psi(t)$ by shifts in the translations and dilations parameters as given below;

$$\Psi_{u,s}(t) = \frac{1}{\sqrt{s}}\Psi\left(\frac{t-u}{s}\right),\ s \neq 0,\ u,s \in R, \tag{1}$$

Where Ψ is known as a mother wavelet and s and u represent the dilation and translation parameters, respectively.

If $f(t)$ is an energy-limited signal then CWT is written as

$$W(u,s) = \frac{1}{\sqrt{s}}\int_{-\infty}^{\infty} f(t)\Psi^*\left(\frac{t-u}{s}\right)dt. \tag{2}$$

In general, signals which are considered for the analysis should be in discrete forms. So, a discrete form of CW and its transform is used [23, 24]. If $A_o(n)$, $n \in Z$ represents a discrete signal of ionospheric TEC so its decomposition can be computed by the following relations;

$$A_j(n) = \sum_{k\in Z} h_k A_{j-1}\left(n - 2^{j-1}k\right), \tag{3}$$

$$D_j(n) = \sum_{k\in Z} g_k D_{j-1}\left(n - 2^{j-1}k\right), \tag{4}$$

where, A_j and D_j represent the discrete approximation and the discrete detail at the jth level or at the resolution of 2^j with respect to A_o, respectively. A_j is called the lower frequency part of signal A_o with a frequency lower than 2^{-j} and D_j is called the higher frequency part of the signal with a frequency lies in the range of 2^{-j} and 2^{-j+1}.

3. RESULTS AND DISCUSSION

Figure 1 shows the variation of the magnitude and obscuration of solar eclipse during its period of occur-

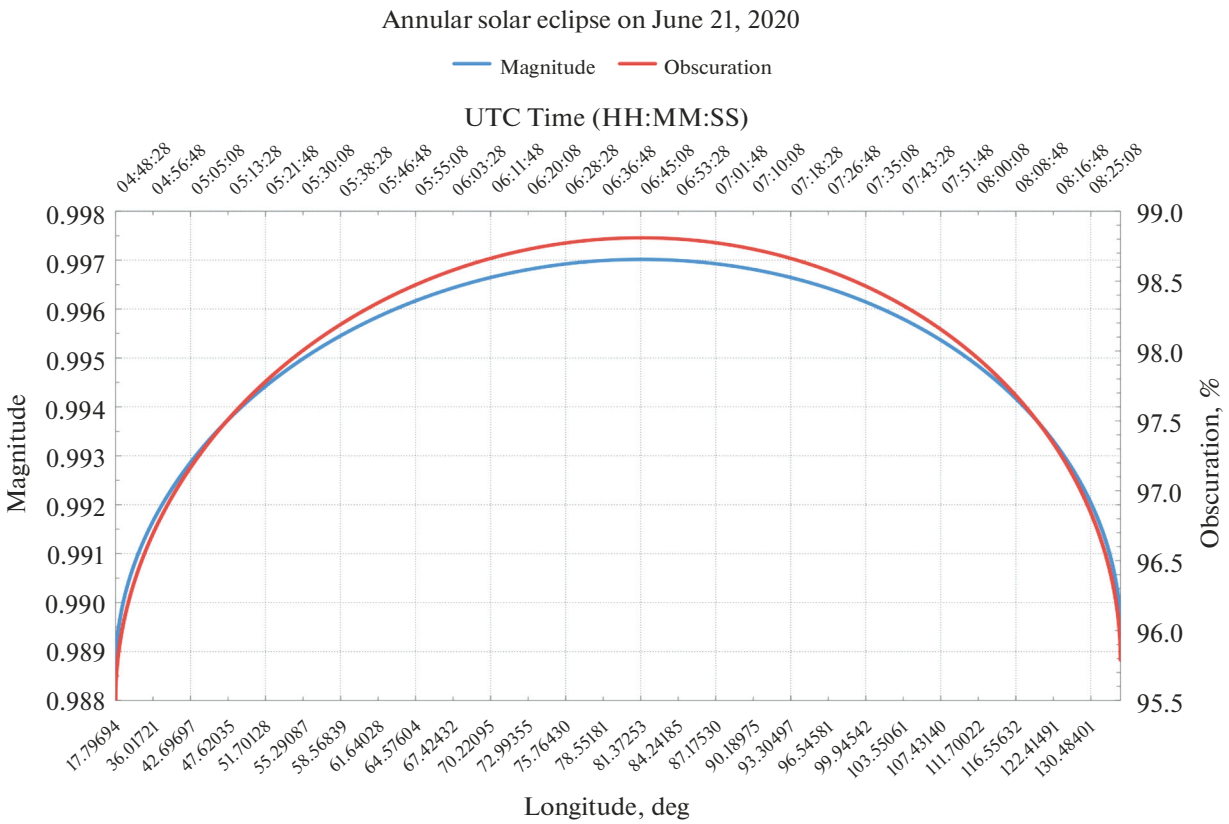

Fig. 1. Shows the variation of the magnitude and obscuration of solar eclipse during its period of occurrence i.e. 09:00–03:30 LT.

rence which are varying from 17.8° to 130.5° longitudes. The maximum values of magnitude and obscuration lie at 81.4° longitude. It can be seen from the figure that all the stations which are considered here (as mentioned in Table 1) lie well on the path of the solar eclipse. The magnitude of the eclipse is defined as the fraction of angular diameter of the celestial body (Sun) which is eclipsed by the moon or it may also be defined as the ratio of the diameter of the sun and the diameter of the moon and its value lies between 0 and 1 for the partial and annular solar eclipse, respectively. It is greater than 1 for the total solar eclipse. The obscuration is the fraction of the Sun's surface area covered by the moon. The magnitude of solar eclipse and obscuration both are different from each other. If the obscuration is 50% then the eclipse magnitude is around 60%. The study of these parameters is extremely important to examine the effect of the solar eclipse on the different observing stations.

Figure 2 represents the diurnal variations of hourly averaged TEC data at different IGS stations including Agra for the period of June, 1–21 2020. The details of the stations under study are mentioned in Table 1. The ranges of latitude and longitude are 9.03°–24.95° N and 38.76°–139.49° E in which stations lie and are covered by the path of the solar eclipse. The white space in the data shows that nonavailability of data. The downward arrow represents the solar eclipse day i.e. June 21. A rectangular box highlights the VTEC variations of eclipse day. This contour plot provides information on how VTEC is varying at all the stations during the period under consideration. The VTEC varies in the range between 2 TECU and 18 TECU. The reductions and enhancements in the data are observed on different days prior (June 9–18) and on the

Table 1. Details of IGS and GPS stations under consideration

Sl. no.	Station codeand country	Locations		Type
		Lat.	Long.	
1	ADIS, Ethiopia	9.03	38.76	IGS
2	DJIG, Djibouti	11.5	42.8	IGS
3	BHR4, Bahrain	26.20	50.6	IGS
4	IISC, India	13.02	77.57	IGS
5	LCK3, India	26.91	80.95	IGS
6	AGRA, India	27.2	78	GPS
7	LHAZ, China	29.65	91.1	IGS
8	BJNM, China	40.25	116.22	IGS
9	GAMG, Republic of Korea	35.59	127.92	IGS
10	KGNI, Japan	35.71	139.49	IGS
11	TWTF, Taiwan	24.95	121.16	IGS

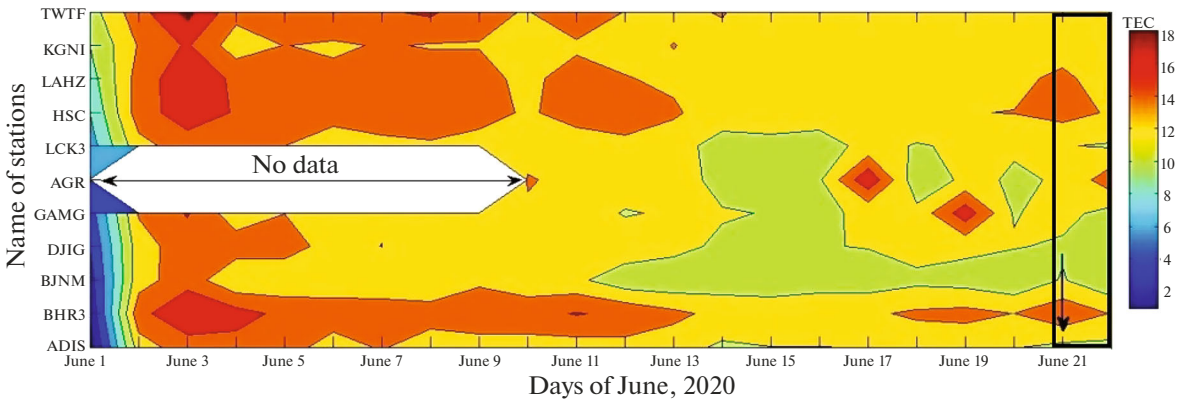

Fig. 2. The contour plot is shown a diurnal variation of TEC data over different IGS stations including GS station Agra during the period of June 1–21, 2020. The downward arrow indicates the day of the solar eclipse, i.e., June 21, 2020.

day of the eclipse (June 21). So it is difficult to prove that the reduction in VTEC variations on June 21 is due to the solar eclipse only. To examine these enhancements and reductions in VTEC variations, the daily average VTEC is plotted for each station separately in Fig. 3. The reductions are found at all the stations except Agra (≈2 TECU), BHR4 (≈1 TECU), and IISC (≈0.5 TECU). The maximum reduction is found at TWTF (≈2 TECU). Although, reductions are also observed on the other days before the solar eclipse i.e. between the range of June 9 and 15, so still we are not able to ascertain that the reduction of June 21 is due to the solar eclipse considered in the present study or it is due to some other factor. To ascertain that the reduction in VTEC variation of June 21 is the result of the solar eclipse, we have investigated per minutes TEC data of all the stations on the day of the solar eclipse for the duration of 09:00 AM to 3:00 PM in which solar eclipse occurred. These variations are shown in Fig. 4. The reductions in the data were clearly observed during the 9:00 AM–3:30 PM except at CKSV, TWTF where relatively enhanced TEC values are observed. Our results are consistent with the results of earlier workers [15, 18, 25]. To examine the solar activity during the period under consideration, solar flux F10.7 and sunspot numbers are plotted in Fig 5a. Sunspot numbers are zero between June 16 and June 21 and F10.7 variations are also decreased in the same period except for a minor enhancement on June 19. On the same front, foF_2 and electron density data of the Agra station have been extracted from the IRI-2016 model which also shows reductions between the period of June 16 and June 21 as shown in Fig. 5b. To examine geomagnetic activity in the period under consideration, geomagnetic activity parameters i.e. ∑Kp and Dst indices are plotted in Fig. 5c. These variations are quiet during the period under consideration which confirms that there is no geomagnetic activity during this period. Moreover, to ascertain the global impact of the eclipse on TEC data we averaged and multiplied the TEC data of all the stations, and then we examined it by using continuous wavelet transforms where two segments of each are plotted. The first segment represents the analyzed signal and the other is the wavelet coefficients. Nonlinear features of TEC data of all the stations can be seen globally i.e. TEC decreases in average and addition but TEC first, increases and then decreases in case of multiplication which can also be seen in the wavelet coefficients plot. These results are shown in Figs. 6a, 6b, respectively. To extract more features of TEC data and to strengthen our results in Fig. 4, wavelet decomposition of the same TEC data (average, addition, and multiplication) is plotted in Figs. 7a, 7b, respectively. The reductions and enhancements in time domain variation of TEC on the eclipse's day followed the same trend in frequency components of the decomposed TEC signals are seen.

The anomalous variations in the TEC data during the solar eclipse explained in terms of different mechanisms are available in the literature [26, 27]. First is the northward magnetic field (**B**) and eastward electric field (**E**) results in E × B drift in the upward direction which drifts the plasma during daytime and is called the equatorial fountain effect [28, 29]. The compressed force is higher at certain altitudes due to the significant influence of gravity which is responsible for the migration of electrons up to 20 deg to the north and south of the equator along with the magnetic field lines. This process results in a decrease in the transport of electrons from the magnetic equator to low latitudes which causes a decrease in TEC variation at the low latitudes and it is greater at middle and high latitudes. [30] explained that the electrons in the crest in the Indonesian region, are controlled by the transportation of electrons from the magnetic equator and also the strength of the fountain effect which is weak during a solar eclipse and results in a decrease in TEC

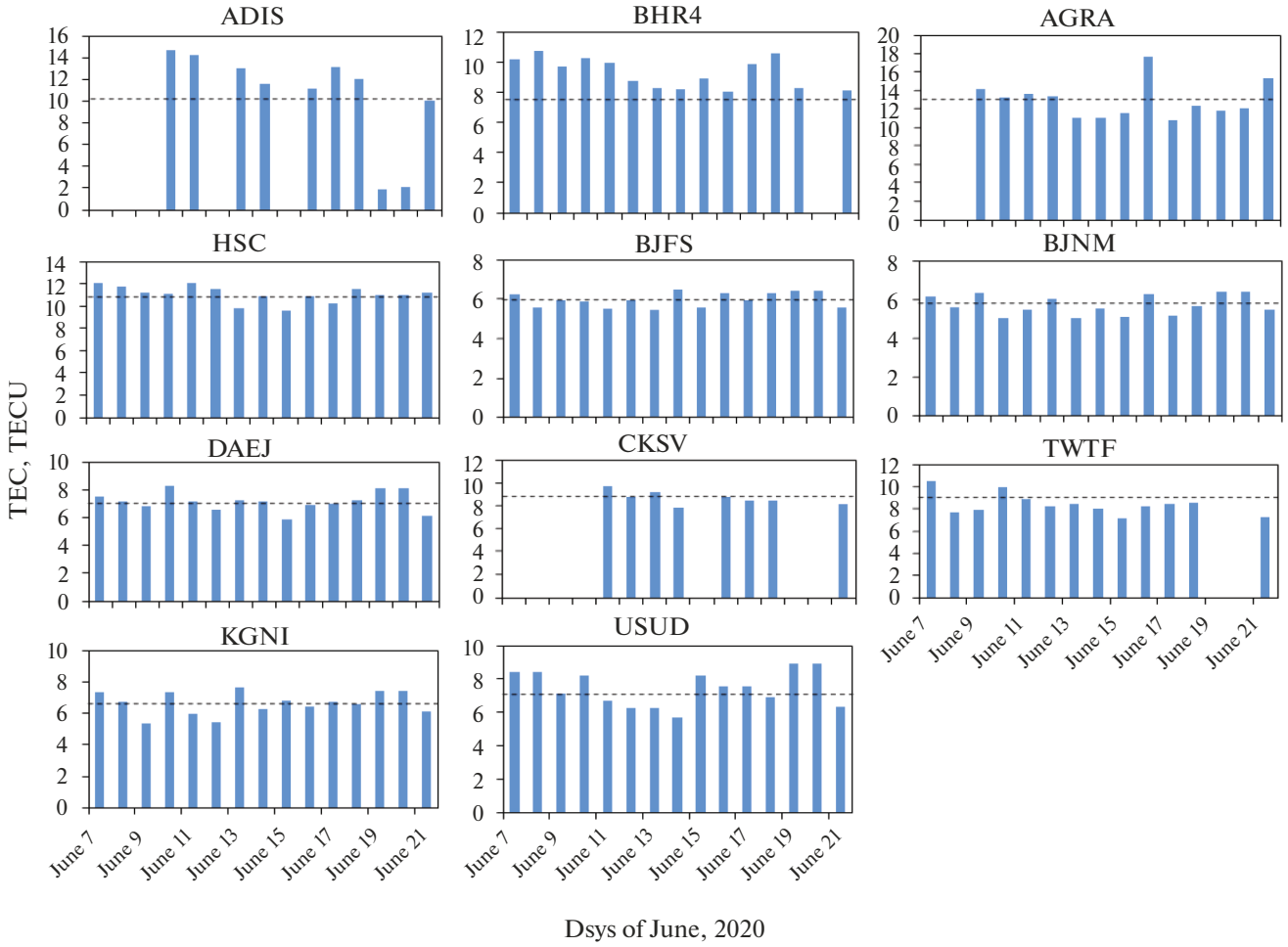

Fig. 3. Plots are represented daily average TEC values of IGS stations (including Agra) for the period of June 7–21, 2020.

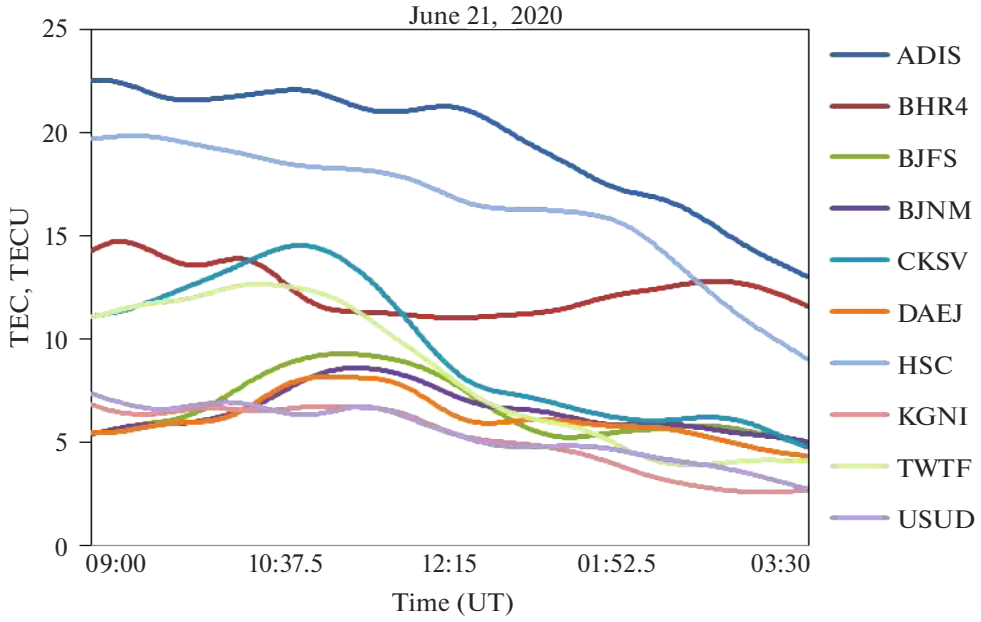

Fig. 4. Variations of TEC are shown for the duration of 09:00–03:30 LT over different IGS stations on June 21, 2020 (Solar eclipse day).

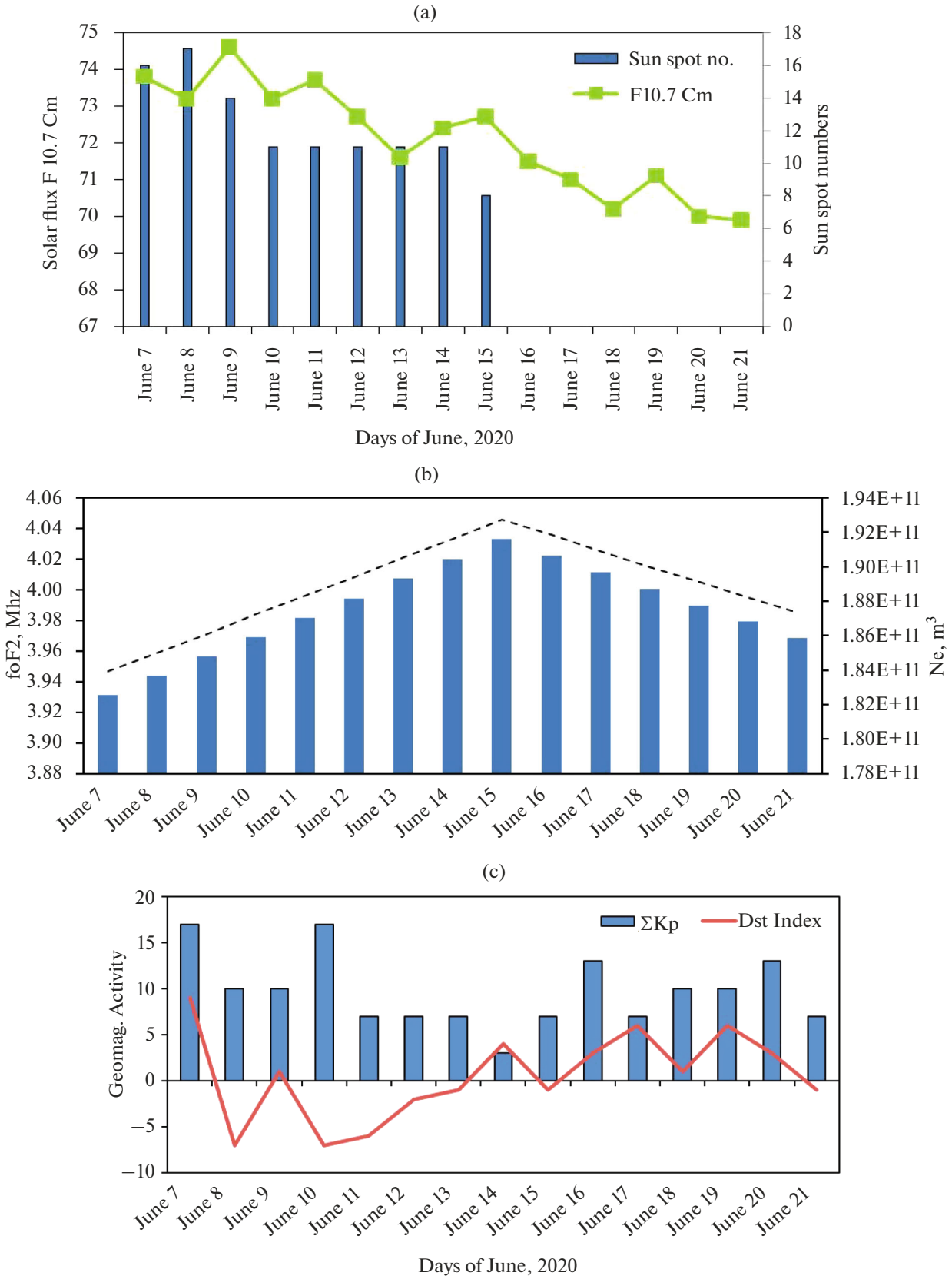

Fig. 5. (a) Variation of solar activity parameters i.e. solar flux F10.7 and sun spot numbers are shown by using solid bars and line respectively for the period under consideration. (b) Variation of foF_2 (MHz) and electron density (Ne, m^{-3}) of the IRI-2016 model are shown by using the dotted line and solid bars respectively for the period June 7–21, 2020. (c) Variation of geomagnetic activity parameters i.e. ∑Kp and Dst indices are shown by using solid bars and solid line respectively for the period under consideration.

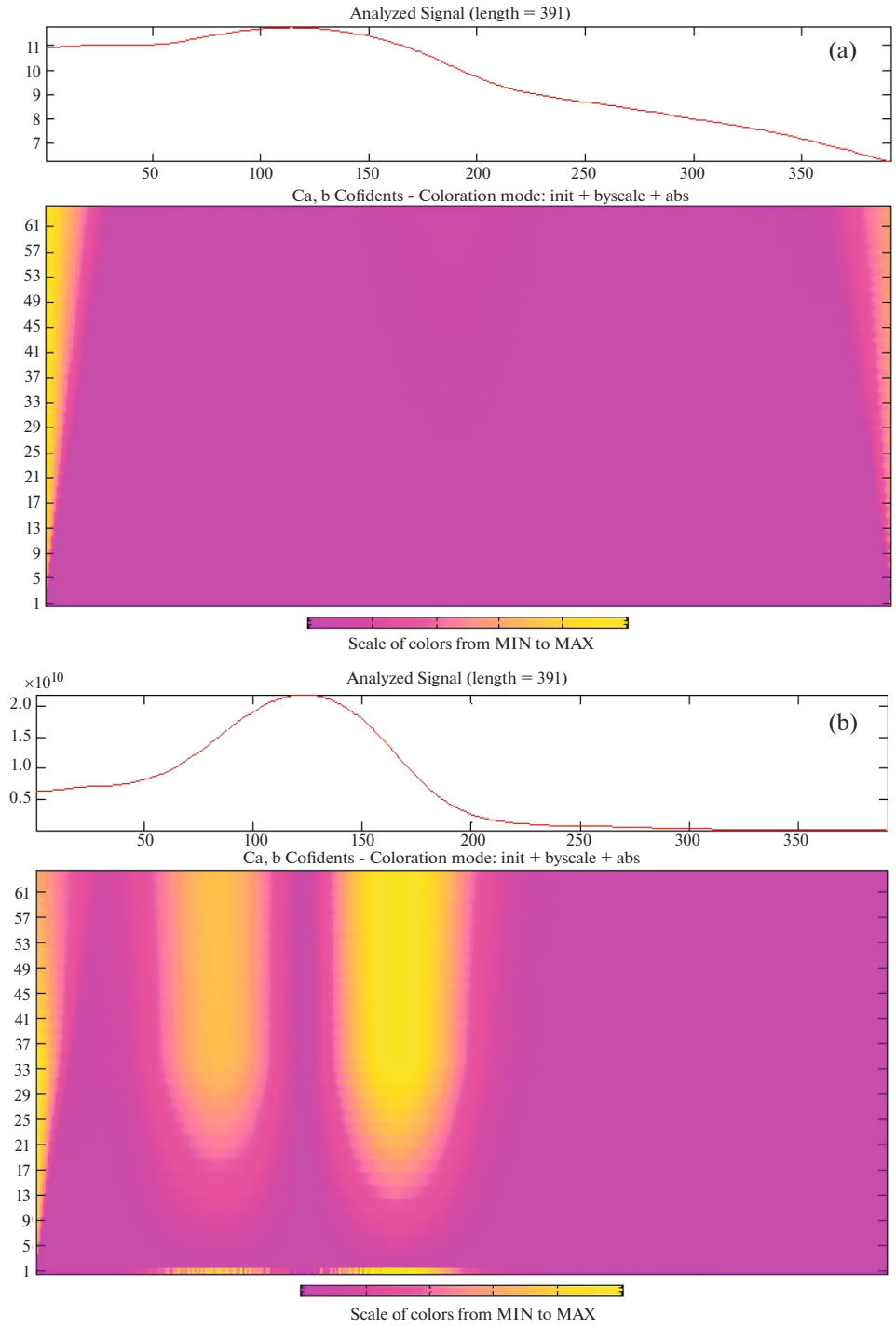

Fig. 6. Continuous wavelet transforms (CWT) of the average, and multiplication of the TEC of all the stations considered is shown for the duration of 09:00-03:30 LT on June 21, 2020 (Solar eclipse's day) in Figs. 6a, 6b, respectively.

variations a few hours to just before the occurrence of the solar eclipse. It may be because of the solar corona obscuration which occurred before the optical disk obscuration. Moreover, the occurrence of early interaction at ionospheric altitudes leads to early interaction on the ground as well. However, a decrement in TEC variation also occurs simultaneously or before the event of the solar eclipse. The decrease in TEC variation is relative to the obscuration of the lunar disc and it is controlled by the electrons which are produced by photoionization [31]. Second is the generation of atmospheric gravity waves (AGWs) during the period of the solar eclipse. The solar eclipse also generates the internal gravity waves in the ionosphere

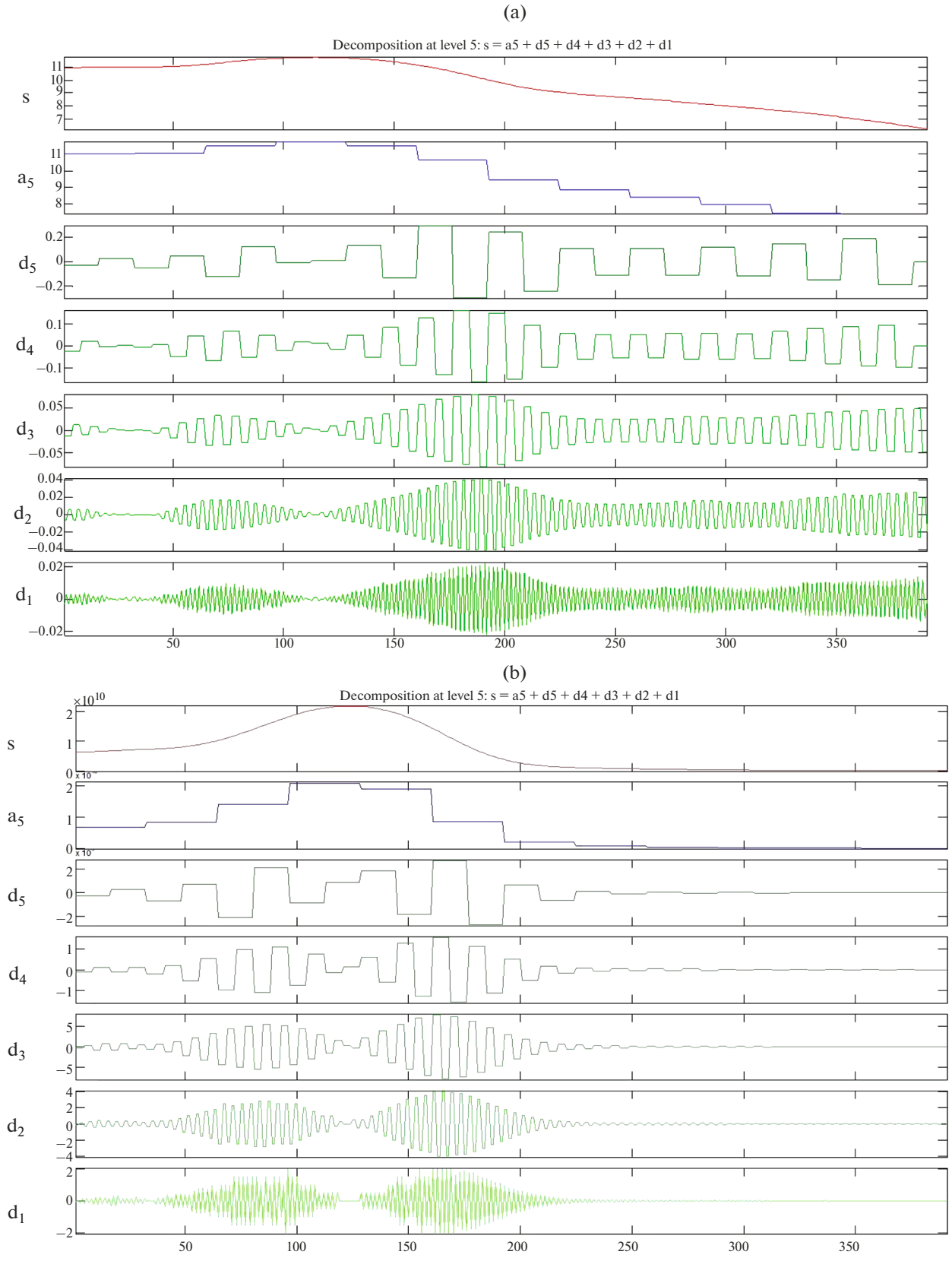

Fig. 7. (a) Wavelet decomposition of the average TEC variation of all the stations is shown for the same duration as shown in Fig. 6. (b) Same as Fig. 7a but for the multiplied TEC variation of all the stations.

which is verified experimentally by many earlier workers [32, 33] and some researchers have done the modeling-based study of the generation of AGWs due to solar eclipse [19, 34]. Now the question arises that how these waves are generated during the event of the f solar eclipse. [35] have shown a schematic representation of how an electric field generates plasma structure by a gravity-wave induced neutral wind and further, they suggested that a wave-induced electric field results in an increase in the drift of ions and electrons in the E_s -layer by E × B drift and it is considered to be the mechanism of low latitude ionosphere.

Our results are also supported by the studies of previous researchers [15, 18, 30, 31]. For example, Ding et al. (2010) have examined the electron density and found a 60% depletion in the F_1 region in central China (26°–36° N, 108°–118° E) during eclipse total obscuration. [36] recorded the variations of hmF_2 and foF_2 by using an ionogram and a 68% depletion was observed in the data in regions adjacent to the dip equator. [37] also detected a significant depletion of TEC (50–60%) along the path of eclipse totality during the great American solar eclipse of August 2017. Recently, [38] examined the behaviour of equatorial ionization anomaly during the solar eclipse of July 2, 2019. They have observed depletion of 35% in TEC in the sub-EIA region along the path of the eclipse totality between ~20:00–21:20 UT and suggested that it is caused by a drastic decrease in photoionization along the solar eclipse totality path within the moon's shadow.

The enhancements in TEC variations during the solar eclipse at AGRA, BHR4, and IISC may be explained in terms of the solar extreme ultraviolet (EUV) which is coupled with the upward vertical E × B drift. The ionization across the magnetic equator is blown by the tidal winds and then TEC is enhanced during nighttime while TEC is depleted because of the small extent of the magnetic flux tubes which stuck the electrons content rapidly after sunset with relation to the lower values of temperatures in the thermosphere during night time [25].

CONCLUSIONS

In the present study, we have analyzed the TEC data recorded at 11 IGS-TEC stations including one GPS station namely Agra corresponding to a solar eclipse of June 21, 2020 for the duration of June 7–21, 2020. The stations are so chosen that all of them lie on the path of eclipse from the beginning to the end. The data have been processed by using statistical and wavelet transform-based techniques. The reductions in the TEC variations are recorded at all the stations except AGRA, BHR4, and IISC. The global impact of the eclipse has been examined over the average, addition, and multiplied TEC data of all the stations by using CWTs and decomposition techniques on the eclipse's day. Our statistical results are well-matched with the wavelet analysis results. The average of TEC variations shows the reduction but in multiplication first, it increases and then decreases. Our results are strengthened by the earlier studies also.

ACKNOWLEDGMENTS

The authors are thankful to the Ministry of Earth Sciences, Government of India, New Delhi for financial support in the form of a major research project. The authors are also thankful to Omniweb NASA for the data of solar flux (F10.7 cm), Sun Spot Numbers, ∑Kp and Dst Indices, and foF_2 and electron density from the IRI-2016 model.

REFERENCES

1. D. Pundhir, B. Singh, O. P. Singh, and S. K. Gupta, "A morphological study of low latitude ionosphere and its implication in identifying earthquake precursors," J. Ind. Geophys. Union **21** (3), 214–222 (2017).
2. A. Paul, T. Das, S. Ray, A. Das, D. Bhowmick, and A. Dasgupta, "Response of the equatorial ionosphere to the total solar eclipse of 22 July 2009 and annular eclipse of 15 January 2010 as observed from a network of stations situated in the Indian longitude sector," Ann. Geophys. **29** (10), 1955–1965 (2011).
3. B. M. Vyas and S. Sunda, "The solar eclipse and its associated ionospheric TEC variations over Indian stations on January 15, 2010," Adv. Space Res. **49**, 546–555 (2012).
4. H. Le, L. Liu, X. Yue, W. Wan, and B. Ning, "Latitudinal dependence of the ionospheric response to solar eclipses," J. Geophys. Res. **114**, A07308 (2009). https://doi.org/10.1029/2009JA014072
5. T. Dang, J. Le, W. Wang, B. Zhang, A. Burns, H. Le, Q. Wu, H. Ruan, X. Dou, and W. Wan, "Global responses of the coupled thermosphere and ionosphere system to the August 2017 Great American Solar Eclipse," J. Geophys. Res.: Space Phys. **123** (8), 7040–7050 (2018).
6. E. T. Burton and E. M. Boardman, "Effects of solar eclipse on audio frequency atmospherics," Nature **131** (3299), 81–82 (1933). https://doi.irg/10.1038/131081a0.
7. P. G. Ledig, M. W. Jones, A. A. Giesecke, and E. J. Chernosky, "Effects on the ionosphere at Huancayo, Peru, of the solar eclipse, January 25, 1944," Terr. Magn. Atmos. Electr. **51** (3), 411–418 (1946). https://doi.org/10.1029/TE051i003p00411
8. G. H. Munro and L. H. Heisler, "Ionospheric records of solar eclipses," J. Atmos. Sol. Terr. Phys. **12** (1), 57–67 (1958). https://doi.org/10.1016/0021-9169(58)90008-4
9. N. Jakowski, S. M. Stankov, V. Wilken, C. Borries, D. Altadill, J. Chum, D. Buresova, J. Boska, P. Sauli, F. Hruska, and L. R. Cander, "Ionospheric behavior over Europe during the solar eclipse of 3 October 2005," J. Atmos. Sol.-Terr. Phys. **70** (6), 836–853 (2008). https://doi.org/10.1016/j.jastp.2007.02.016

10. F. Ding, W. Wan, B. Ning, L. Liu, H. Le, G. Xu, M. Wang, G. Li, Y. Chen, Z. Ren, B. Xiong, L. Hu, X. Yue, B. Zhao, F. Li, et al., "GPS TEC response to the 22 July 2009 total solar eclipse in East Asia," J. Geophys. Res. **115**, 1–8 (2010).
11. M. K. M. Haridas and G. Manju, "On the response of the ionospheric F region over Indian low-latitude station Gadanki to the annular solar eclipse of 15 January 2010," J. Geophys. Res. **117**, A01302, 1–7 (2012). https://doi.org/10.1029/2011JA016695
12. J. D. Huba and D. Drob, "SAMI3 prediction of the impact of the 21 August 2017 total solar eclipse on the ionosphere/plasmasphere system," Geophys. Res. Lett. **44**, 5928–5935 (2017).
13. S. M. Stankov, N. Bergeot, D. Berghmans, D. Bolsee, C. Bruyninx, et al., "Multi-instrument observations of the solar eclipse on 20 March 2015 and its effects on the ionosphere over Belgium and Europe," J. Space Weather Space Clim. **7** (A19) (2017). https://doi.org/10.1051/swsc/2017017
14. I. Cherniak and I. Zakharenkova, "Ionospheric total electron content response to the Great American Solar Eclipse of 21 August 2017," Geophys. Res. Lett. **45**, 1199–1208 (2018).
15. V. Dear, A. Husin, S. Anggarani, J. Harjosuwito, and R. Pradipta, "Ionospheric effects during the total solar eclipse over Southeast Asia-Pacific on 9 March 2016: Part 1. Vertical movement of plasma layer and reduction in electron plasma density," J. Geophys. Res.: Space Phys. **125** (5), e2019JA026708 (2020).
16. N. R. Nelli, M. Temimi, R. Fonseca, D. Francis, O. Nesterov, R. Abida, M. Weston, and A. Kumar, "Anatomy of the annular solar eclipse of 26 December 2019 and its impact on land–atmosphere interactions over an arid region," IEEE Geosci. Remote Sens. Lett. **2020**, 1–5 (2020). https://doi.org/10.1109/LGRS.2020.3003084
17. O. N. Boitman, A. D. Kalikhman, and A. V. Tashchilin, "The mid-latitude ionosphere during the total solar eclipse of March 9, 1997," J. Geophys. Res. **104**, 28197–28206 (1999).
18. H. Le, L. Liu, X. Yue, and W. Wan, "The midlatitude F2 layer during solar eclipses: Observations and modeling," J. Geophys. Res. **113**, A08309 (2008).
19. S.-R. Zhang, P. J. Erickson, L. P. Goncharenko, A. J. Coster, W. Rideout, and J. Vierinen, "Ionospheric bow waves and perturbations induced by the 21 August 2017 solar eclipse," Geophys. Res. Lett. **44**, 12067–12073 (2017).
20. W. Srigutomo, A. Singarimbun, W. Meutia, I. Gede Putu Fadjar Soerya Djaja, B. Muslim, and P. Abadi, "Decrease of total electron content during the 9 March 2016 total solar eclipse observed at low latitude stations, Indonesia," Ann. Geophys. (2019). https://doi.org/10.5194/angeo-2019-11
21. S. Mallat, "Zero-crossings of a wavelet transform," IEEE Trans. Inf. Theory **37**, 1019–1033 (1991).
22. L. He, L. Wu, S. Pulinets, S. Liu, and F. Yang, "A nonlinear background removal method for seismo-ionospheric anomaly analysis under a complex solar activity scenario: A case study of the M9.0 Tohoku earthquake," Adv. Space Res. **50**, 211–220 (2012).
23. A. Grossman and J. Morlet, "Decomposition of Hardy functions into square integrable wavelets of constant shape," SIAM J. Math. Anal. **15** (4), 726–736 (1984).
24. M. L. Hilton, "Wavelet and wavelet packet compression of electrocardiograms," IEEE Trans. Biomed. Eng. **44** (5), 394–402 (1997).
25. S. Kumar, A. K. Singh, and R. P. Singh, "Ionospheric response to total solar eclipse of 22 July 2009 in different Indian regions," Ann. Geophys. **31** (9), 1549–1558 (2013).
26. T. Dang, J. H. Lei, W. B. Wang, M. D. Yan, D. X. Ren, and F. Q. Huang, "Prediction of the thermospheric and ionospheric responses to the 21 June 2020 annular solar eclipse," Earth Planet. Phys. **4**, pp. 231–237 (2020).
27. G. Uma, P. S. Brahmanandam, V. K. D. Srinivasu, D. S. V. V. D. Prasad, V. S. Gowtam, T. S. Ram, and Y. H. Chud, "Ionospheric responses to the 21 August 2017 great American solar eclipse: A multi-instrument study," Adv. Space Res. **65** (1), 74–85 (2019).
28. E. V. Appleton, "Two anomalies in the ionosphere," Nature **157**, 691–691 (1946). https://doi.org/10.1038/157691a0
29. M. C. Kelley, B. G. Fejer, and C. A. Gonzales, "An explanation for anomalous equatorial ionospheric electric fields associated with a northward turning of the interplanetary magnetic field," J. Geophys. Res. **6** (4), 301–304 (1979).
30. A.-H. Chen, S.-B. Yu, and J.-S. Xu, "Ionospheric response to a total solar eclipse deduced by the GPS Beacon observations," Wuhan Univ. J. Nat. Sci. **4** (4), 439–444 (1999).
31. S. Kumar and A. K. Singh, "Changes in total electron content (TEC) during the annular solar eclipse of 15 January 2010," Adv. Space Res. **49**, 75–82 (2012).
32. G. Chimonas and C. O. Hines, "Atmospheric gravity waves induced by a solar Eclipse," J. Geophys. Res. **75**, 857–875 (1970).
33. M. J. Davis and A. V. Da Rosa, "Possible detection of atmospheric gravity waves generated by the solar eclipse," Nature **226**, 1123 (1970).
34. D. C. Fritts and Z. Luo, "Gravity wave forcing in the middle atmosphere due to reduced ozone heating during a solar eclipse," J. Geophys. Res., **98**, pp. 3011–3021 (1993).
35. Y. H. Chu, P. S. Brahmanandam, C. Y. Wang, and C. L. Su, "Coordinated observations of sporadic E using Chung-Li 30 MHz radar ionosonde and FORMOSAT 3/COSMIC satellites," J. Atmos. Sol. Terr. Phys. **73**, 883–894 (2010).
36. J. O. Adeniyi, S. M. Radicella, I. A. Adimula, A. A. Willoughby, O. A. Oladipo, and O. Olawepo, "Signature of the 29 March 2006 eclipse on the ionosphere over an equatorial station," J. Geophys. Res. **112** (A6), A06314 (2007).
37. A. J. Coster, L. Goncharenko, S. Zhang, P. J. Erickson, W. Rideout, and J. Vierinen, "GNSS observations of ionospheric variations during the 21 August 2017 solar eclipse," Geophys. Res. Lett. **17**, 349–352 (2017).
38. O. F. Jonah, L. Goncharenko, P. J. Erickson, S. Zhang, A. Coster, J. L. Chau, E. R. de Paula, and W. Rideout, "Anomalous behavior of the equatorial ionization anomaly during the July 2, 2019 solar eclipse," J. Geophys. Res. **125**, 1–12 (2020).